arXiv:1606.07866v3 [hep-th] 12 Jan 2017

Holographic Metal-Insulator Transition in Higher Derivative Gravity

Yi Ling [1,3],* Peng Liu [1],† Jian-Pin Wu [2,3],‡ and Zhenhua Zhou [1§]

[1] *Institute of High Energy Physics,*
Chinese Academy of Sciences, Beijing 100049, China

[2] *Institute of Gravitation and Cosmology,*
Department of Physics, School of Mathematics and Physics,
Bohai University, Jinzhou 121013, China

[3] *Shanghai Key Laboratory of High Temperature Superconductors, Shanghai, 200444, China*

Abstract

We introduce a Weyl term into the Einstein-Maxwell-Axion theory in four dimensional spacetime. Up to the first order of the Weyl coupling parameter γ, we construct charged black brane solutions without translational invariance in a perturbative manner. Among all the holographic frameworks involving higher derivative gravity, we are the first to obtain metal-insulator transitions (MIT) when varying the system parameters at zero temperature. Furthermore, we study the holographic entanglement entropy (HEE) of strip geometry in this model and find that the second order derivative of HEE with respect to the axion parameter exhibits maximization behavior near quantum critical points (QCPs) of MIT. It testifies the conjecture in [1, 2] that HEE itself or its derivatives can be used to diagnose quantum phase transition (QPT).

*lingy@ihep.ac.cn

†Corresponding author. liup51@ihep.ac.cn

‡jianpinwu@mail.bnu.edu.cn

§zhouzh@ihep.ac.cn

I. INTRODUCTION

Quantum phase transition (QPT) [3] occurs at absolute zero temperature when varying system parameters, which is believed to account for some peculiar phenomena observed in novel condensed matter at finite temperature, such as the strange metal. As a fundamental issue in condensed matter physics, QPT has attracted a lot of interest of both theorists and experimentalists. However, QPT usually involves strong correlation physics where conventional perturbative techniques lose the power.

Recently, gauge/gravity duality [4–6] has provided a novel mechanism to implement QPT in holographic approach, especially metal-insulator transition (MIT), for instance see recent review [7] and references therein. One key ingredient of implementing MIT in holography is to introduce the momentum dissipation by breaking the translational symmetry, meanwhile deform the near horizon geometry to new IR fixed point which is dual to an insulating phase [8, 9]. A simple holographic model with momentum dissipation can be constructed by introducing a set of massless axion fields [10]. In its original version, only the metallic phase was found. Later, when a general potential of axions or an additional dilaton field is introduced into this Einstein-Maxwell-Axion (EMA) model, the insulating phase has also been observed [11–16]. Recent investigation on the hydrodynamic and transport properties of EMA model without translational invariance can be found, for instance in [17–19].

In this paper, we provide a new strategy to implement MIT by introducing higher-derivative terms into the EMA model. This is also the first time realizing MIT in the framework of higher derivative gravity. In four dimensional spacetime, there are eight independent terms in a general four-derivative action [20], which may emerge as quantum corrections in the low energy effective action of superstring theory [21, 22]. From the viewpoint of the dual conformal field theory (CFT), these terms correspond to the corrections of finite 't Hooft coupling and/or beyond the large-N limit. Here, we only focus on a special term with coupling between gauge field and the Weyl tensor, which has been dubbed as Weyl term [20, 23, 24]. In holographic literature, it has been shown that the presence of the Weyl term in four-dimensional Schwarzschild-AdS geometry induces non-trivial behavior of the conductivity in dual theory [20], in contrast to the frequency-independent conductivity without Weyl term [25]. Specifically, the real part of the conductivity displays a peak or a valley near zero frequency which depends on the sign of Weyl coupling parameter, implying

that the frequency-dependent conductivity is particle-like or vortex-like, respectively [20] (also see [26–30]).

Once the Weyl term is taken into account, the equations of motion for this Einstein-Maxwell-Axion-Weyl (EMA-Weyl) theory become a set of third order differential equations with high nonlinearity, which is very hard to solve analytically so far. As the first step, we treat the Weyl coupling parameter γ as a small number and construct analytical solutions up to the first order of this parameter. This strategy has previously been used to construct perturbative charged black hole solutions for high-derivative gravity in [23, 31–35]. With the background solutions up to $\mathcal{O}(\gamma)$, we will study the thermodynamics of the dual field theory. Moreover, the direct current (DC) conductivity can be derived analytically, which allows us to study the phase structure at zero temperature directly. We will demonstrate that MIT as a quantum critical phenomenon can be observed in this circumstance manifestly.

Stimulated by our recent work [1, 2], we intend to investigate the behavior of holographic entanglement entropy (HEE) close to QPT in this holographic model. In condensed matter physics, a lot of work have revealed that the entanglement itself or its derivatives displays local extremes close to QCPs [36–46]. Nevertheless, this phenomenon calls for deeper theoretical understanding. Recently our series of work [1, 2] have disclosed that the HEE or its first order derivatives with respect to system parameters can be used to characterize the QPT such that a holographic description of the relation between EE and QPT has been established. We have also proposed that it should be a universal feature that the HEE or its derivatives with respect to system parameters can diagnose the QPT in a generic holographic framework. The robustness of this proposal awaits for further test. Therefore, it is very natural to ask whether the quantum critical phenomena observed in this model can also be captured by HEE. Interestingly enough, in this paper we will demonstrate that the *second* order derivative of HEE does exhibit maximization behavior close to QCPs. This observation not only justifies the conjecture in [1, 2], but also enriches our understanding on the scenario of HEE characterizing QPT.

Our paper is organized as follows. We shall firstly introduce a Weyl term into four dimensional EMA theory and then obtain the perturbative black hole solutions in Section II, with a brief discussion on the thermodynamics of the background. In Section III, we calculate DC conductivity of the dual system at absolute zero temperature and then demonstrate that MIT takes place as quantum critical dynamics. Then we move on to the study of the HEE

in Section IV and show that the second order derivative of HEE with respect to system parameter exhibits peaks close to QPTs. In Section V, we summarize the results of this paper and discuss some open questions for further investigation.

II. EINSTEIN-MAXWELL-AXIONS-WEYL MODEL

A. Setup and equations of motion

We consider a four dimensional EMA theory with an additional Weyl term coupled to the Maxwell field (EMA-Weyl model), whose action reads as

$$S=\int d^4x\sqrt{-g}\left[R+6-\frac{1}{4}F_{\mu\nu}F^{\mu\nu}-\sum_{I=x,y}(\partial\phi_I)^2+\gamma C_{\mu\nu\rho\sigma}F^{\mu\nu}F^{\rho\sigma}\right], \tag{1}$$

where $F=dA$ and γ is the Weyl coupling parameter. ϕ_I is a set of free massless axion fields, responsible for the momentum dissipation [10]. $C_{\mu\nu\rho\sigma}$ is the Weyl tensor, which is defined as

$$C_{\mu\nu\rho\sigma}=R_{\mu\nu\rho\sigma}-(g_{\mu[\rho}R_{\sigma]\nu}-g_{\nu[\rho}R_{\sigma]\mu})+\frac{1}{3}Rg_{\mu[\rho}g_{\sigma]\nu}. \tag{2}$$

It is straightforward to derive the equations of motion from the action in (1), which read as

$$\Box\phi_I=0\,, \tag{3}$$

$$\nabla_\mu[F^{\mu\nu}-4\gamma C^{\mu\nu\rho\sigma}F_{\rho\sigma}]=0\,, \tag{4}$$

$$\begin{aligned}&R_{\mu\nu}-\frac{1}{2}Rg_{\mu\nu}-3g_{\mu\nu}-\frac{1}{2}\Big(F_{\mu\rho}F_\nu{}^\rho-\frac{1}{4}g_{\mu\nu}F_{\rho\sigma}F^{\rho\sigma}\Big)-\partial_\mu\phi_x\partial_\nu\phi_x+\frac{g_{\mu\nu}}{2}(\partial\phi_x)^2\\&-\partial_\mu\phi_y\partial_\nu\phi_y+\frac{g_{\mu\nu}}{2}(\partial\phi_y)^2-\gamma(G_{1\mu\nu}+G_{2\mu\nu}+G_{3\mu\nu})=0\,,\end{aligned} \tag{5}$$

where

$$G_{1\mu\nu}=\frac{1}{2}g_{\mu\nu}R_{\alpha\beta\rho\sigma}F^{\alpha\beta}F^{\rho\sigma}-3R_{(\mu|\alpha\beta\lambda|}F_{\nu)}{}^\alpha F^{\beta\lambda}-2\nabla_\alpha\nabla_\beta(F^\alpha_{(\nu}F^\beta_{\mu)})\,, \tag{6}$$

$$\begin{aligned}G_{2\mu\nu}=&-g_{\mu\nu}R_{\alpha\beta}F^{\alpha\lambda}F^\beta_\lambda+g_{\mu\nu}\nabla_\alpha\nabla_\beta(F^\alpha_\lambda F^{\beta\lambda})+\Box(F_\mu{}^\lambda F_{\nu\lambda})-2\nabla_\alpha\nabla_{(\mu}(F_{\nu)\beta}F^{\alpha\beta})\\&+2R_{\nu\alpha}F_\mu{}^\beta F^\alpha_\beta+2R_{\alpha\beta}F^\alpha_\mu F^\beta_\nu+2R_{\alpha\mu}F^{\alpha\beta}F_{\nu\beta}\,,\end{aligned} \tag{7}$$

$$G_{3\mu\nu}=\frac{1}{6}g_{\mu\nu}RF^2-\frac{1}{3}R_{\mu\nu}F^2-\frac{2}{3}RF^\alpha_\mu F_{\alpha\nu}+\frac{1}{3}\nabla_{(\nu}\nabla_{\mu)}F^2-\frac{1}{3}g_{\mu\nu}\Box F^2\,. \tag{8}$$

As pointed out in the introduction, it is difficult to solve this system with full backreaction. Next we intend to construct a perturbative charged black brane solution to this system up to $\mathcal{O}(\gamma)$.

B. Charged black brane solutions

In this subsection, we intend to construct a charged black brane solutions by solving above equations (3), (4) and (5). To this end, we take the following ansatz,

$$\begin{aligned} ds^2 &= -r^2 f(r) dt^2 + \frac{1}{r^2 f(r)} dr^2 + r^2 g(r)(dx^2 + dy^2)\,, \\ A &= A_t(r) dt\,, \quad \phi_x = kx\,, \quad \phi_y = ky\,, \end{aligned} \tag{9}$$

where the UV boundary is located at $r \to \infty$. A non-zero $A_t(r)$ is introduced for a finite chemical potential. The special form of ϕ_I in (9) retains homogeneity as well as isotropy of spacetime but dissipates the momentum of the UV boundary CFT. k is the system parameter and also is referred to as axionic charge. This model does not have manifest lattice wave vector but captures features of disorder, which is characterized by the axionic charge k [12, 16, 47].

Since the equations of motion for the axion fields ϕ_I in (3) are not influenced by the corrections from Weyl term, we only need to expand the functions $f(r)$, $g(r)$ and $A_t(r)$ in powers of γ up to the first order,

$$\begin{aligned} f(r) &= f_0(r) + \gamma Y(r)\,, \\ g(r) &= 1 + \gamma G(r)\,, \\ A_t(r) &= A_{t0}(r) + \gamma H(r)\,, \end{aligned} \tag{10}$$

where $f_0(r)$ and $A_{t0}(r)$ are leading order solutions, while $G(r)$, $H(r)$ and $Y(r)$ are corrections of order $\mathcal{O}(\gamma)$.

These functions can be determined by directly solving the equations of motion (3), (4) and (5) to the zeroth and first order of γ,

$$f_0(r) = 1 - \frac{M}{r^3} + \frac{q^2}{r^4} - \frac{k^2}{r^2}\,, \tag{11}$$

$$A_{t0}(r) = \mu - \frac{2q}{r}\,, \tag{12}$$

$$G(r) = \frac{4q^2}{9r^4} - \frac{g_0}{r} + g_1\,, \tag{13}$$

$$H(r) = \frac{296q^3}{45r^5} - \frac{4Mq}{r^4} - \frac{16k^2 q}{9r^3} - \frac{g_0 q}{r^2}\,, \tag{14}$$

$$Y(r) = -\frac{104q^4}{45r^8} + \frac{20Mq^2}{9r^7} - \frac{32q^2}{9r^4} + \frac{20k^2q^2}{9r^6} + \frac{g_0 q^2}{r^5} - \frac{g_0 M}{2r^4} + \frac{g_1 k^2}{r^2} - \frac{g_0}{r}\,. \tag{15}$$

Eqs. (11) and (12) are exactly the solutions of EMA model proposed in [10]. In above equations, there are five integration constants (μ, q, M, g_0, g_1), which are not independent from one another. Subsequently, we shall derive the relations among these parameters.

First, one can show that the integration constants g_0 and g_1 can be eliminated by coordinate transformations $r \to r + \gamma g_0/2,\ x \to x(1-\gamma g_1/2),\ y \to y(1-\gamma g_1/2)$ as well as a redefinition of the axion charge $k \to k(1+\gamma g_1/2)$. Then, up to $\mathcal{O}(\gamma)$ Eqs. (11 - 15) can be reexpressed as

$$\begin{aligned}
f_0(r) &= 1 - \frac{M}{r^3} + \frac{q^2}{r^4} - \frac{k^2}{r^2}\,, \\
A_{t0}(r) &= \mu - \frac{2q}{r}\,, \\
G(r) &= \frac{4q^2}{9r^4}\,, \\
H(r) &= \frac{296q^3}{45r^5} - \frac{4Mq}{r^4} - \frac{16k^2q}{9r^3}\,, \\
Y(r) &= -\frac{104q^4}{45r^8} + \frac{20Mq^2}{9r^7} - \frac{32q^2}{9r^4} + \frac{20k^2q^2}{9r^6}\,.
\end{aligned} \tag{16}$$

Furthermore, the location of the horizon r_h of this Weyl corrected charged black brane solutions is determined by

$$f(r_h) = 0\,. \tag{17}$$

In the mean time, to guarantee that A is well-defined on the horizon, we need to set

$$A_t(r_h) = 0\,. \tag{18}$$

We can refer above two conditions as the horizon conditions, which give the relations among (μ, q, M) as

$$q = \frac{r_h\mu}{2} + \gamma\Big(\frac{29\mu^3}{180r_h} - r_h\mu + \frac{5k^2\mu}{9r_h}\Big)\,, \tag{19}$$

$$M = \frac{r_h\mu^2}{4} + r_h^3 - k^2 r_h + \gamma\Big(\frac{7\mu^4}{45r_h} - \frac{4r_h\mu^2}{3} + \frac{5k^2\mu^2}{9r_h}\Big)\,. \tag{20}$$

And then it is straightforward to derive the Hawking temperature of this black brane as

$$T = -\frac{4k^2 + \mu^2 - 12r_h^2}{16\,(\pi r_h)} + \gamma\frac{(\mu^4 - 60\mu^2 r_h^2)}{720\pi r_h^3}\,. \tag{21}$$

Note that we have expanded all the above quantities q, M and T to $\mathcal{O}(\gamma)$.

C. Thermodynamics

In this subsection, we briefly discuss the thermodynamics of the quantum field theory dual to the EMA-Weyl system with a standard approach (see e.g. [48]). To this end, we first construct the renormalized action S_{ren} by adding a boundary term to the original action (1) as

$$S_{ren} = S + S_{bdy} = S + \int_{r\to\infty} dx^3\sqrt{h}(2\mathcal{K} - 4)\,, \tag{22}$$

where h is the determinant of the induced metric h_{ij} on the boundary and $\mathcal{K}$ is the trace of the extrinsic curvature on slice with constant r. By a straightforward calculation, the free energy density can be derived as

$$F = \left(-\frac{1}{4}\mu^2 r_h - r_h^3 - k^2 r_h\right) + \gamma\left(-\frac{7\mu^4}{45r_h} + \frac{4\mu^2 r_h}{3} - \frac{5k^2\mu^2}{9r_h}\right)\,. \tag{23}$$

And then, we derive the charge density Q, entropy density s, pressure P and energy density ϵ as

$$Q = -\frac{\partial F}{\partial \mu} = \mu r_h + \frac{\gamma\left(-180\mu r_h^2 + 100k^2\mu + 29\mu^3\right)}{90r_h}\,, \tag{24}$$

$$s = -\frac{\partial F}{\partial T} = 4\pi r_h^2 - \frac{20}{9}\gamma\left(\pi\mu^2\right)\,, \tag{25}$$

$$P = -F = \left(\frac{1}{4}\mu^2 r_h + r_h^3 + k^2 r_h\right) + \gamma\left(\frac{7\mu^4}{45r_h} - \frac{4\mu^2 r_h}{3} + \frac{5k^2\mu^2}{9r_h}\right)\,, \tag{26}$$

$$\epsilon = 2r_h^3 + \frac{\mu^2 r_h}{2} - 2k^2 r_h + \frac{\gamma\left(-120\mu^2 r_h^2 + 50k^2\mu^2 + 14\mu^4\right)}{45r_h}\,. \tag{27}$$

where $\epsilon = sT + \mu Q - P$ [48] has been used in the last equation. Again, all above thermodynamical quantities are obtained up to $\mathcal{O}(\gamma)$.

One can also check that s and ϵ are the Wald entropy density [49] and ADM mass density respectively [50, 51]. In addition, for vanishing axions, *i.e.*, $k = 0$, our results agree with that in [33, 34].

III. METAL-INSULATOR TRANSITION

In this section we study the MIT by analyzing the behavior of direct current (DC) conductivity. By definition, a MIT is reflected by an abrupt change of DC conductivity behavior, which is a macroscopic observable governed by quantum critical physics. To be more specific, at zero temperature, the DC conductivity of a metallic phase behaves as $\partial_T\sigma_{DC} < 0$,

while for insulating phase, it behaves as $\partial_T \sigma_{DC} > 0$. Then the critical point (line) of MIT is determined by $\partial_T \sigma_{DC} = 0$. Therefore, to demonstrate the MIT from EMA-Weyl model, we shall firstly calculate the DC conductivity in what follows.

In the calculation of DC conductivity, it is more readily adapted to work in coordinate $z \equiv r_h/r$. Note that for a given γ, the Weyl corrected EMA black hole solutions are parametrized by two scaling-invariant parameters, $\hat{k} \equiv k/\mu$ and $\widehat{T} \equiv T/\mu$. With these in mind, we rewrite the background solutions as follows

$$\begin{aligned} ds^2 &= \frac{1}{z^2}\Big[-f(z)dt^2 + \frac{1}{f(z)}dz^2 + g(z)(dx^2+dy^2)\Big]\,, \\ A &= A_t(z)dt\,, \end{aligned} \tag{28}$$

where $f(z)$, $g(z)$ and $A_t(z)$ now take the form as

$$\begin{aligned} f(z) =& (1-z)p(z)\,, \qquad g(z) = 1+\gamma\frac{\mu^2 z^4}{9}, \\ p(z) =& \gamma\frac{\mu^2 z^3}{180}[240+100\hat{k}^2\mu^2(z^3-1)+2\mu^2(13z^4-14)+(\mu^2-100)(z^3+z^2+z)] \\ &+1+z+(1-\hat{k}^2\mu^2)z^2-\frac{\mu^2}{4}z^3, \\ A_t(z) =& \mu\Big[(1-z)+\gamma\frac{z}{90}\big(180+20\hat{k}^2\mu^2(-5-4z^2+9z^3)-29\mu^2+74\mu^2z^4-45z^3(4+\mu^2)\big)\Big]\,. \end{aligned} \tag{29}$$

Also the dimensionless Hawking temperature $\hat{T} \equiv T/\mu$, which is given by

$$\hat{T} = \frac{12-\mu^2-4\hat{k}^2\mu^2}{16\pi\mu} + \gamma\frac{\mu(\mu^2-60)}{720\pi}\,. \tag{30}$$

Now, we calculate the DC conductivity in dual field theory employing the scheme proposed in [52] (also see [53]). We turn on a constant electric field from the beginning, instead of an alternating current (AC) electric field. Specifically, we take the following consistent ansatz

$$\delta A_x = -E_x t + a_x(z)\,, \quad \delta g_{tx} = \frac{1}{z^2}[h_{tx}(z)+\gamma G(z)h_{tx}(z)]\,, \quad \delta\phi_x = \chi_x(z)\,. \tag{31}$$

The key point of this method is to find the conserved current in the bulk [52, 53], which is in this model

$$J^x = \sqrt{-g}(F^{zx} - 4\gamma C^{zx\alpha\beta}F_{\alpha\beta})\,. \tag{32}$$

Up to $\mathcal{O}(\gamma)$, J^x can be expressed as

$$J^x = -Qh_{tx} + fa_x' - \frac{2}{3}\gamma z^2 f a_x' f''\,. \tag{33}$$

Here we have denoted $J^t = Q$, which is the conserved electric charge density. The DC conductivity can then be obtained from the following expression

$$\sigma_{DC} = \frac{J^x}{E_x}\,. \tag{34}$$

As revealed in [52, 53], given a conserved current J^x along the radial direction, it is enough to determine the DC conductivity from the requirement of the regularity of the perturbation variables at the horizon $z = 1$. We illuminate this procedure in what follows.

First, to have a well defined gauge field at the horizon, we have

$$a_x'(z) = \frac{E_x}{f(z)}\,. \tag{35}$$

Second, when the momentum conservation is violated, h_{tx} should be finite at the horizon and we can extract this value from the $t - x$ component of Einstein equation, which reads after taking value at $z = 1$

$$h_{tx}\Big[6(-6 + 2k^2 + f'(-4 + \gamma G') + f'') + A_t'^2(-3 + 8\gamma f' - 4\gamma f'')\Big] - 2f a_x' A_t'(3 + 4\gamma f'') = 0\,. \tag{36}$$

And finally, combining Eqs. (32), (35) and (36), the DC conductivity can be expressed as a function of $(\hat{k}, \mu, \gamma)$,

$$\sigma = 1 + \frac{1}{2\hat{k}^2} + \gamma\Big(4 - \frac{8}{3}\hat{k}^2\mu^2 + \frac{\mu^2}{9} + \frac{\frac{4}{15}\mu^2 - 2}{\hat{k}^2}\Big)\,. \tag{37}$$

Armed with (37), we study the MIT by examining the behavior of σ in zero temperature limit. First, we directly see from (37) that when $\gamma = 0$, the DC conductivity is independent of the temperature, which has been observed in [10]. But when $\gamma \neq 0$, the DC conductivity is temperature dependent (Fig. 1). In particular, we find that given a nonzero γ, a MIT occurs when varying the system parameter $\hat{k}$ (see the left plot in Fig.2). To demonstrate the MIT of this model more explicitly, we plot the phase diagram over $(\gamma, \hat{k})$ plane at zero temperature in Fig.2 (right plot). The quantum critical line (blue line in the right plot in Fig.2) is determined by $\partial_{\hat{T}}\sigma_{DC} = 0$ at zero temperature, as is discussed at the beginning of this section, which corresponds to $\hat{k} = \frac{1}{4}\sqrt{\frac{1}{15}(5 + \sqrt{5785})} \simeq 0.58116$. This quantum critical line is independent of γ. Specifically, we observe that for $\gamma > 0$, the transition from metallic phase to insulating phase occurs when increasing $\hat{k}$. For $\gamma < 0$, however, the opposite scenario is obtained.

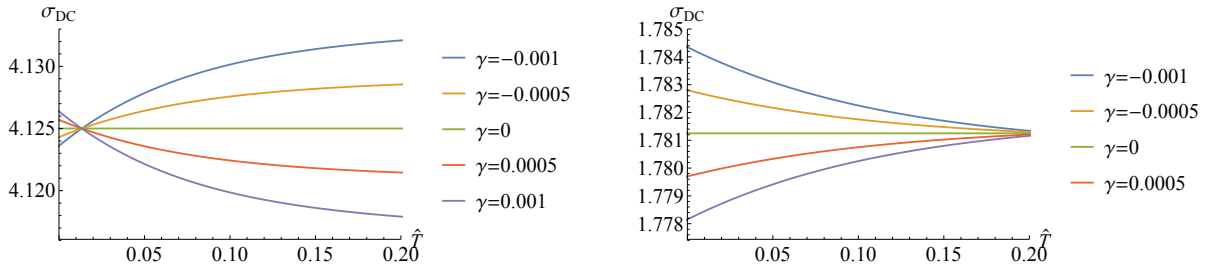

FIG. 1: The DC conductivity σ_{DC} as the function of the temperature $\hat{T}$ for some specific $\hat{k}$ (left plot for $\hat{k} = 0.4$ and right plot for $\hat{k} = 0.8$) and γ.

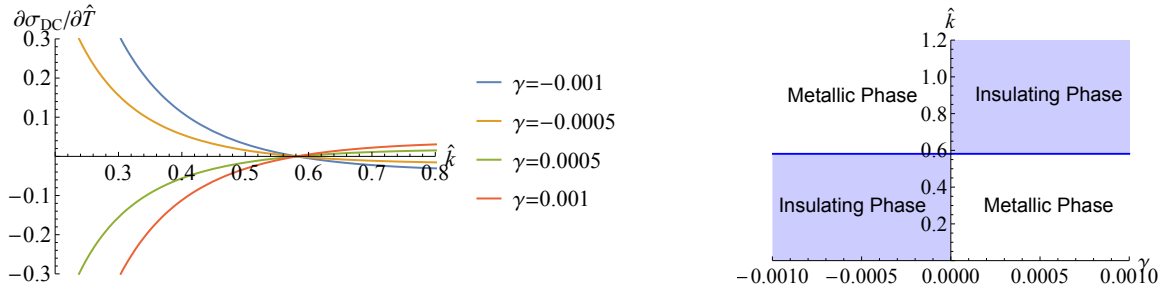

FIG. 2: Left plot: $\partial_{\hat{T}}\sigma_{DC}$ as a function of $\hat{k}$ at zero temperature for different Weyl parameters γ. Right plot: The phase diagram over $(\gamma, \hat{k})$ plane for the MIT at zero temperature in the Weyl corrected EMA geometry. The transverse blue line corresponds to the critical line $\hat{k} \simeq 0.58116$. Note that $\gamma \neq 0$ here.

In [20, 26–30], the transport behavior of the boundary field theory dual to Schwarzschild-AdS geometry has been studied. The optical conductivity near the zero frequency displays a Drude-like peak for $\gamma > 0$, while for $\gamma < 0$ the conductivity exhibits a valley near zero frequency. As argued in [20] (also see [26–30]), the Drude-like behavior for $\gamma > 0$ could be described by the collision and motion of charged particles, while the valley behavior for $\gamma < 0$ should be depicted by the collision of vortices. Further, it is revealed in [20, 26–30] that for small γ, an EM duality-transformation relates the equations of motions of the Maxwell field at γ and the one at $-\gamma$, leading to $\sigma(\omega, \gamma) \simeq 1/\sigma(\omega, -\gamma)$ in the dual boundary theory. Later, a broader class of particle-vortex duality was revealed in [54, 55], which is different from that in [20, 26–30]. From Fig. 1 we find that in our model $\sigma_{DC}(\gamma, T)$ exhibits an interesting mirror symmetry

$$\sigma_{DC}(\gamma, T) \simeq const. - \sigma_{DC}(-\gamma, T), \tag{38}$$

when $\hat{k}$ is fixed, which can be viewed as a special particle-vortex duality as investigated in [54, 55]. It can be deduced from Eq.(38) that $\partial_T\sigma(\gamma, T)$ is an odd function of γ, which is also numerically depicted in the left plot of Fig.2. Thus, we have a "metal-insulator" duality when changing the sign of γ, as illustrated in the right plot of Fig.2. A concrete and analytical derivation of Eq.(38) in our present model, however, would be more complicated and difficult than that in [20, 26–30] due to the involvement of finite charge density and momentum dissipation. We leave this issue for future investigation.

Our present holographic EMA-Weyl model is dual to a boundary field theory with finite density and momentum dissipation. For weak momentum dissipation (small k), the transport behaves as metallic for $\gamma > 0$, which may be described by the motion and collision of particles [20]. With the increase of $\hat{k}$ the motion of particles is suppressed and the system undergoes a phase transition from a metallic phase to an insulating phase. It is deduced from Eq.(38) that an opposite scenario happens for $\gamma < 0$, which results in the phase structure as illustrated in the right plot of Fig. 2.

IV. HOLOGRAPHIC ENTANGLEMENT ENTROPY CLOSE TO QCPS

In this section, we study the HEE for the dual field theory living on the boundary. It has been revealed in [1, 2] that HEE or its first order derivative with respect to system parameters exhibit local extremes near QCPs, and thus can be used to diagnose QPT in holographic framework. It is also conjectured in [2] that higher-order derivatives of HEE probably play a similar role in characterizing QPT in holographic models. Inspired by this observation, we intend to compute the HEE in our present model. In comparison with the previous holographic models with MIT, one nice feature of our current model is that analytical solutions for black brane with zero temperature are derived such that we can directly compute the HEE in a bulk geometry at zero temperature.

Before calculating the HEE explicitly, it is worthwhile to point out a key difference in the holographic description of EE in higher derivative gravity. It is noticed that the original Ryu-Takayanagi formula [56, 57] only holds for Einstein gravity. In [58], an alternative prescription for HEE is proposed for Lovelock gravity. This prescription reproduces the universal contribution to the EE for the dual CFT in four and six dimensional spacetimes. Further, a general formula for HEE in higher derivative gravity is proposed in [59]. This

formula includes the Wald entropy as the leading term and a correction from extrinsic curvature, which is usually dubbed as the anomaly term of HEE. For our model, it is easy to check that the anomaly term of HEE vanishes for the Weyl corrected action (1). Therefore, on a slice with fixed time, it is valid to calculate the HEE of our present model with the leading term of the formula proposed in [59], which is

$$S_{EE} = -2\pi \int_{\Sigma} d^2x\sqrt{h}\frac{\partial \mathcal{L}}{\partial R_{\mu\nu\rho\sigma}}\varepsilon_{\mu\nu}\varepsilon_{\rho\sigma}\,, \tag{39}$$

where $\mathcal{L}$ is the Lagrangian density of action (1), $\varepsilon_{\mu\nu}$ is the Levi-Civita symbol, and h is determinant of the induced metric on the surface Σ that minimizes the functional S_{EE}. In this EMA-Weyl model, the formula (39) can be evaluated as

$$S_{EE} = 4\pi \int_{\Sigma} d^2x\sqrt{h}\Big(1+\frac{1}{3}\gamma F^2\Big). \tag{40}$$

Now we compute the HEE in a bulk geometry at zero temperature. We consider a strip geometry on the dual boundary system that has length $L_y \to \infty$ in y-direction and finite width $\hat{l}$ in x-direction. Given the fact that both h and F are functions of radial axis z only, we can label the Σ with the location of its bottom z_* in z-direction. Since the boundary is asymptotically AdS_4, the S_{EE} for each background solution will receive a vacuum contribution. Here we define the HEE as $\hat{S} \equiv (S_{EE} - S_{vac})/2\pi L_y$ with vacuum contribution S_{vac} subtracted out. The scaling-invariant width l and HEE S can be expressed as,

$$S = \frac{4}{\mu}\left(\frac{1}{z_*} + \int_0^{z_*} dz\left[\frac{(\gamma F^2(z)+3)^2 g_{yy}(z)\sqrt{g_{xx}(z)g_{zz}(z)}}{3\sqrt{\xi}} - \frac{1}{z^2}\right]\right), \tag{41}$$

$$l = 2\mu \int_0^{z_*} dz\left(\gamma F^2(z_*)+3\right)\sqrt{\frac{g_{xx}(z_*)\,g_{yy}(z_*)\,g_{zz}(z)}{g_{xx}(z)\xi}}, \tag{42}$$

where $l = \mu\hat{l}$, $S = \hat{S}/\mu$, and $\xi \equiv (\gamma F^2(z)+3)^2 g_{xx}(z)g_{yy}(z) - (\gamma F^2(z_*)+3)^2 g_{xx}(z_*)\,g_{yy}(z_*)$.

Next we study the relation between the HEE and QPT in this Weyl corrected EMA model. Notice that in scenario of HEE characterizing QPT, the first order derivative to HEE [2] or the HEE itself [1] characterizes the QPT with local extremes near QCPs. Nevertheless, in present model, the HEE itself as well as its first derivative are featureless. Instead, we find that the second order derivative of HEE with respect to system parameter $\hat{k}$ exhibits peaks near the critical points of the MIT. As we can see from Fig. 3, $\partial^2 S/\partial\hat{k}^2$ reaches its local extreme near the critical $k_c = 0.58116$, regardless of the value of γ. To demonstrate

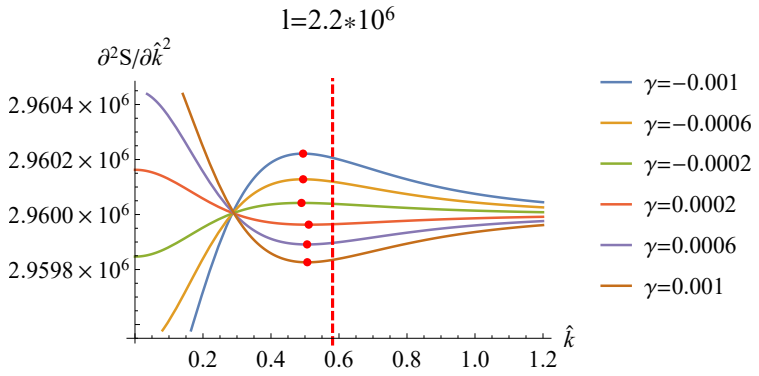

FIG. 3: Each curve represents the $\partial^2 S/\partial\hat{k}^2$ *v.s.* $\hat{k}$ with γ specified by the plot legends. The red dashed line is $\hat{k}_c = 0.58116$.

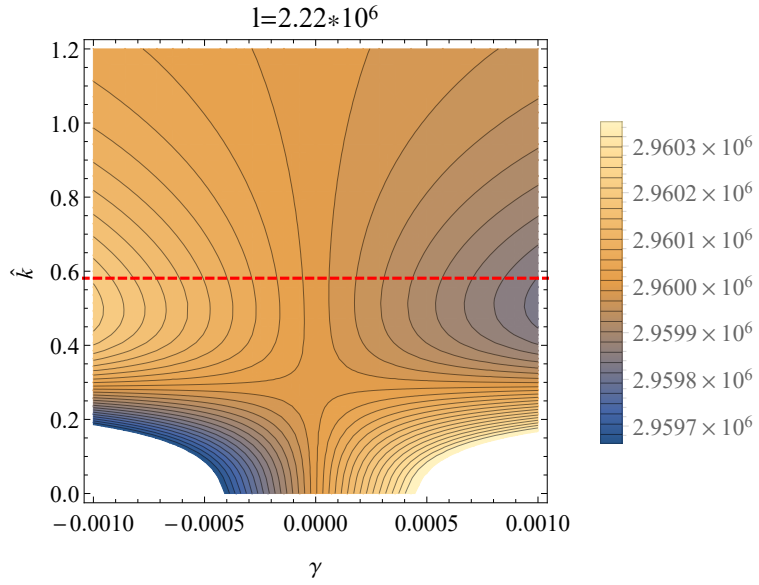

FIG. 4: The contour plot of $\partial^2 S/\partial\hat{k}^2$ over $(\gamma, \hat{k})$ at $l = 2.22\times10^6$ and $\hat{T} = 0$. The values of $\partial^2 S/\partial\hat{k}^2$ can be read from the plot legends. The red dashed curve is the quantum critical line shown in Fig. 2.

this phenomenon more transparently, we show the contour plot of $\partial^2 S/\partial\hat{k}^2$ over the $(\gamma, \hat{k})$ in Fig. 4. From this plot it is easily seen that the local extremes (ridge for $\gamma < 0$ and valley for $\gamma > 0$) of $\partial^2 S/\partial\hat{k}^2$ is close to the quantum critical line. We would like to point out that the connection between the $\partial^2 S/\partial\hat{k}^2$ and the critical line is prominent only for $l > 10^5$. The bigger the l is, the better the $\partial^2 S/\partial\hat{k}^2$ diagnoses the QPT. This phenomenon is a natural result since the quantum critical properties, which emerge at large scale, are

expected to be captured by large scale HEE. Specially, in the limit of large l we find that the S/l converges to the Wald entropy density s, indicating that s is also a good indicator of the MIT in the present holographic model. Similar phenomenon has been observed in [1] as well. This phenomenon is in accordance with CMT result that the entanglement measure characterizing the QPT becomes more prominent with the increase of block size l.

Finally, it is noticed that there exists a mild discrepancy between the ridge/valley and the quantum critical line. One peculiar feature of our model is that the Wald entropy density is non-zero for both metallic and insulating phases even at zero temperature, thus the thermal contribution to HEE can not be ignored and its effect to such a discrepancy is unclear. At this stage we propose that mutual information, which subtracts out the thermal contribution from the HEE, might play a better role in diagnosing the QPT. We intend to study this in future.

V. DISCUSSIONS AND OPEN QUESTIONS

In this paper, we have constructed perturbative black brane solutions to EMA-Weyl gravity model and studied the electrical transport properties. A MIT is observed in our model, that is the first realization of MIT in holographic models with higher derivative gravity. We have also investigated the relation between HEE and MIT, and found that the second order derivative of HEE with respect to system parameter $\hat{k}$ exhibits peaks or valleys near the critical points of MIT. Our results further testifies the conjecture in [1, 2] and enriches the scenario of HEE characterizing QPTs. Certainly, it can be expected that HEE characterizing QPT with even higher orders of derivatives could be observed in holographic models. These two results are of crucial importance to a comprehensive understanding of quantum critical phenomena and the long-standing question in CMT - why and how the EE characterize the QPT.

After a series of work on the relation between HEE and QPT, it becomes urgent to understand the underlying reasons that lead to different derivative orders of HEE diagnosing the QPT in holographic approach, which is also an open problem in CMT. Previously, it was argued in CMT literature for instance in [60] that the derivative order of entanglement which becomes extremal or divergent might be related the order of the QPT, which is determined by the behavior of free energy of the system. Based on our results, however, this

correspondence is not observed in holographic framework. Nevertheless, it is instructive to summarize and compare what we have observed in this series of work.

1. In [1], HEE itself exhibits local extremes near the QCPs of the MIT. The ground state entropy density is *vanishing* for insulating phases, while *nonvanishing* for the metallic phase, reflecting an AdS_2 near horizon geometry.

2. In [2], it is the first order derivative of HEE with respect to the system parameter that diagnoses the QCPs of the MIT. In this circumstance both metallic phase and insulating phase have *vanishing* ground state entropy density.

3. In present paper, the second order derivative of HEE with respect to the relevant parameter $\hat{k}$ characterizes the QPT. Correspondingly, both metallic phase and insulating phase have *nonvanishing* ground state entropy density.

Therefore we intend to propose that the derivative order of HEE which signals QPT might be related to the behavior of ground state entropy density in holographic approach. We also expect that a well-designed quantity that removes the thermal contribution from HEE, for instance the mutual information [61], might play a crucial role in unveiling the relation between the derivative order of HEE and the QPT. We leave all these important issues for further study. Next we point out some other interesting topics worthy of further investigation.

First, it would be interesting to incorporate the holographic superconductor into our current framework. In [62], the Weyl corrected holographic superconductor without backreaction is constructed. An important feature is that the ratio ω_g/T_c of gap frequency ω_g over critical temperature T_c of superconducting phase transition runs with the Weyl parameter γ. In particular, when $\gamma < 0$, the value of ω_g/T_c is lower than that $\omega_g/T_c \simeq 8$ in the usual holographic superconductor [63–65]. These results have been confirmed in subsequent series of works, see for example [66–73]. It would be interesting to see how the ratio ω_g/T_c is affected by the γ and $\hat{k}$ in our model.

Another worthwhile improvement to our current work is to obtain black brane solutions with full backreaction, which involves solving the differential equations beyond the second order. Although our results are robust, but the first order approximation requires the γ to be very small. Solutions with full backreaction will allow us to explore the properties of the

system at wider range of γ. When full backreaction is considered, the following important issues could be addressed. First, our present perturbative EMA-Weyl background has AdS_2 IR geometry at zero temperature, which associates with a finite ground state entropy density. It would be valuable to examine the behavior of the ground state entropy density with the full backreaction. Second, the computation of optical conductivity with full backreaction will reflect a more accurate phase structure. Furthermore, we could study further the mild discrepancy between the ridge of the HEE and the critical line when the full backreaction is considered. In addition, it is also interesting to include the superconductor in our present model with full backreaction.

Finally, we would like to point out that it is sobering to realize that our model may suffer from the micro-causality violation and the instability of the dual CFT because of the introduction of the higher derivative term in action (1) [24, 74, 75]. By analyzing the causality of the CFT dual to the Schwarzschild-AdS geometry and the stabilities of the vector modes, a constraint is placed on γ [20, 24]. While the backreaction of higher derivative term is included, the causality and the stability should be reexamined. In this situation, however, we need to turn on not only vector modes but also scalar and tensor modes to analyze their causality and stability, and the resulting equations are much more complicated than [20, 24]. At this stage, we leave the rigorous analysis for future investigation.

Acknowledgements

We are very grateful to Wei-Jia Li for helpful discussion. This work is supported by the Natural Science Foundation of China under Grant Nos.11275208, 11305018 and 11575195, and by the grant (No. 14DZ2260700) from the Opening Project of Shanghai Key Laboratory of High Temperature Superconductors. Y.L. also acknowledges the support from Jiangxi young scientists (JingGang Star) program and 555 talent project of Jiangxi Province. J. P. Wu is also supported by the Program for Liaoning Excellent Talents in University (No. LJQ2014123).

---

[1] Y. Ling, P. Liu, C. Niu, J. P. Wu and Z. Y. Xian, JHEP04(2016)114 [arXiv:1502.03661 [hep-th]].

[2] Y. Ling, P. Liu and J. P. Wu, Phys. Rev. D **93**, no. 12, 126004 (2016) [arXiv:1604.04857 [hep-th]].

[3] S. Sachdev, *Quantum Phase Transitions,* (Cambridge University Press, Cambridge, 2000).

[4] J. M. Maldacena, Int. J. Theor. Phys. **38**, 1113 (1999) [Adv. Theor. Math. Phys. **2**, 231 (1998)] [hep-th/9711200].

[5] E. Witten, Adv. Theor. Math. Phys. **2**, 253 (1998) [hep-th/9802150].

[6] S. S. Gubser, I. R. Klebanov and A. M. Polyakov, Phys. Lett. B **428**, 105 (1998)

[7] Y. Ling, Int. J. Mod. Phys. A **30**, no. 28&29, 1545013 (2015).

[8] A. Donos and S. A. Hartnoll, Nature Phys. **9**, 649 (2013) [arXiv:1212.2998].

[9] A. Donos and J. P. Gauntlett, JHEP **1404**, 040 (2014) [arXiv:1311.3292 [hep-th]].

[10] T. Andrade and B. Withers, JHEP **1405**, 101 (2014) [arXiv:1311.5157 [hep-th]].

[11] M. Baggioli and O. Pujolas, Phys. Rev. Lett. **114**, no. 25, 251602 (2015) [arXiv:1411.1003 [hep-th]].

[12] M. Baggioli and O. Pujolas, arXiv:1601.07897 [hep-th].

[13] M. Baggioli and O. Pujolas, arXiv:1604.08915 [hep-th].

[14] E. Kiritsis and J. Ren, JHEP **1509**, 168 (2015) [arXiv:1503.03481 [hep-th]].

[15] B. Goutéraux, JHEP **1404**, 181 (2014) [arXiv:1401.5436 [hep-th]].

[16] B. Goutéraux, E. Kiritsis and W. J. Li, JHEP **1604**, 122 (2016) [arXiv:1602.01067 [hep-th]].

[17] Y. Ling, Z. Y. Xian and Z. Zhou, arXiv:1605.03879 [hep-th].

[18] L. Cheng, X. H. Ge and Z. Y. Sun, JHEP **1504**, 135 (2015) [arXiv:1411.5452 [hep-th]].

[19] Y. L. Wang and X. H. Ge, arXiv:1605.07248 [hep-th].

[20] R. C. Myers, S. Sachdev and A. Singh, Phys. Rev. D **83**, 066017 (2011) [arXiv:1010.0443 [hep-th]].

[21] K. Hanaki, K. Ohashi and Y. Tachikawa, Prog. Theor. Phys. **117**, 533 (2007) [hep-th/0611329].

[22] S. Cremonini, K. Hanaki, J. T. Liu and P. Szepietowski, JHEP **0912**, 045 (2009) [arXiv:0812.3572 [hep-th]].

[23] R. C. Myers, M. F. Paulos and A. Sinha, JHEP **0906**, 006 (2009) [arXiv:0903.2834 [hep-th]].

[24] A. Ritz and J. Ward, Phys. Rev. D **79**, 066003 (2009) [arXiv:0811.4195 [hep-th]].

[25] C. P. Herzog, P. Kovtun, S. Sachdev and D. T. Son, Phys. Rev. D **75**, 085020 (2007) [hep-th/0701036].

[26] W. Witczak-Krempa and S. Sachdev, Phys. Rev. B **86**, 235115 (2012) [arXiv:1210.4166 [cond-

mat.str-el]].

[27] W. Witczak-Krempa and S. Sachdev, Phys. Rev. B **87**, 155149 (2013) [arXiv:1302.0847 [cond-mat.str-el]].

[28] W. Witczak-Krempa, E. Sorensen and S. Sachdev, Nature Phys. **10**, 361 (2014) [arXiv:1309.2941 [cond-mat.str-el]].

[29] W. Witczak-Krempa, Phys. Rev. B **89**, no. 16, 161114 (2014) [arXiv:1312.3334 [cond-mat.str-el]].

[30] R. C. Myers, T. Sierens and W. Witczak-Krempa, arXiv:1602.05599 [hep-th].

[31] J. T. Liu and P. Szepietowski, Phys. Rev. D **79**, 084042 (2009) [arXiv:0806.1026 [hep-th]].

[32] R. G. Cai and D. W. Pang, Phys. Rev. D **84**, 066004 (2011) [arXiv:1104.4453 [hep-th]].

[33] A. Dey, S. Mahapatra and T. Sarkar, JHEP **1601**, 088 (2016) [arXiv:1510.00232 [hep-th]].

[34] A. Dey, S. Mahapatra and T. Sarkar, arXiv:1512.07117 [hep-th].

[35] S. Mahapatra, JHEP **1604**, 142 (2016) [arXiv:1602.03007 [hep-th]].

[36] L. Amico, R. Fazio, A. Osterloh and V. Vedral, Rev.Mod.Phys. **80**, 517 (2008) [arXiv:0703044 [quant-ph]].

[37] Y. Chen, Z. Wang, and F. Zhang, Phys. Rev. B **73**, 224414 [arXiv:quant-ph/0512143].

[38] A. Hamma, W. Zhang, S. Haas, and D. A. Lidar, Phys. Rev. B **77**, 155111 (2008) [arXiv:0705.0026 [quant-ph]].

[39] A. Osterloh, L. Amico, G. Falci, R. Fazio, Nature **416**, 608 (2002) [arXiv:0202029 [quant-ph]]

[40] T. J. Osborne and M. A. Nielsen, Phys. Rev. A **66**, 032110 (2002) [arXiv:0202162 [quant-ph]].

[41] G. Vidal, J. Latorre, E. Rico, A. Kitaev. Phys. Rev. Lett. **90**, 227902 (2003) [arXiv:0211074 [quant-ph]].

[42] Y. Chen, P. Zanardi, Z. D. Wang and F. C. Zhang, New J. Phys. **8**, 97 (2006).

[43] A. Anfossi, P. Giorda, A. Montorsi, and F. Traversa, Phys. Rev. Lett. **95**, 056402 (2005) [arXiv:cond-mat/0502500].

[44] L.-A. Wu, M. S. Sarandy, D. A. Lidar, and L. J. Sham, Phys. Rev. A **74**, 052335 [arXiv:quant-ph/0512031].

[45] L.-A. Wu, M. S. Sarandy, and D. A. Lidar, Phys. Rev. Lett. **93**, 250404.

[46] D. Larsson and H. Johannesson, Phys. Rev. Lett. **95**, 196406.

[47] S. Grozdanov, A. Lucas, S. Sachdev and K. Schalm, Phys. Rev. Lett. **115**, no. 22, 221601 (2015) [arXiv:1507.00003 [hep-th]].

[48] S. A. Hartnoll, Class. Quant. Grav. **26**, 224002 (2009)

[49] R. M. Wald, Phys. Rev. D **48**, 3427 (1993) doi:10.1103/PhysRevD.48.R3427 [gr-qc/9307038].

[50] A. Ashtekar and A. Magnon, Class. Quant. Grav. **1**, L39 (1984).

[51] A. Ashtekar and S. Das, Class. Quant. Grav. **17**, L17 (2000) [hep-th/9911230].

[52] A. Donos and J. P. Gauntlett, JHEP **1406**, 007 (2014) [arXiv:1401.5077 [hep-th]].

[53] M. Blake and A. Donos, Phys. Rev. Lett. **114**, no. 2, 021601 (2015) [arXiv:1406.1659 [hep-th]].

[54] C. P. Burgess and B. P. Dolan, Phys. Rev. B **63**, 155309 (2001) [hep-th/0010246].

[55] J. Murugan and H. Nastase, arXiv:1606.01912 [hep-th].

[56] S. Ryu and T. Takayanagi, Phys. Rev. Lett. **96**, 181602 (2006) [hep-th/0603001].

[57] S. Ryu and T. Takayanagi, JHEP **0608**, 045 (2006) [hep-th/0605073].

[58] L. Y. Hung, R. C. Myers and M. Smolkin, JHEP **1104**, 025 (2011) [arXiv:1101.5813 [hep-th]].

[59] X. Dong, JHEP **1401**, 044 (2014) [arXiv:1310.5713 [hep-th]].

[60] D. Larsson and H. Johannesson, Phys. Rev. A **73**, 042320 (2006)

[61] S. Kundu and J. F. Pedraza, arXiv:1602.07353 [hep-th].

[62] J. P. Wu, Y. Cao, X. M. Kuang and W. J. Li, Phys. Lett. B **697**, 153 (2011) [arXiv:1010.1929 [hep-th]].

[63] S. A. Hartnoll, C. P. Herzog and G. T. Horowitz, Phys. Rev. Lett. **101**, 031601 (2008) [arXiv:0803.3295 [hep-th]].

[64] G. T. Horowitz and M. M. Roberts, Phys. Rev. D **78**, 126008 (2008) [arXiv:0810.1077 [hep-th]].

[65] S. A. Hartnoll, C. P. Herzog and G. T. Horowitz, JHEP **0812**, 015 (2008) [arXiv:0810.1563 [hep-th]].

[66] D. Z. Ma, Y. Cao and J. P. Wu, Phys. Lett. B **704**, 604 (2011) [arXiv:1201.2486 [hep-th]].

[67] D. Momeni and M. R. Setare, Mod. Phys. Lett. A **26**, 2889 (2011) [arXiv:1106.0431 [physics.gen-ph]].

[68] D. Momeni, N. Majd and R. Myrzakulov, Europhys. Lett. **97**, 61001 (2012) [arXiv:1204.1246 [hep-th]].

[69] Z. Zhao, Q. Pan and J. Jing, Phys. Lett. B **719**, 440 (2013) [arXiv:1212.3062].

[70] D. Momeni, R. Myrzakulov and M. Raza, Int. J. Mod. Phys. A **28**, 1350096 (2013) [arXiv:1307.8348 [hep-th]].

[71] D. Momeni, M. Raza and R. Myrzakulov, Int. J. Geom. Meth. Mod. Phys. **13**, 1550131 (2016) [arXiv:1410.8379 [hep-th]].

[72] L. Zhang, Q. Pan and J. Jing, Phys. Lett. B **743**, 104 (2015) [arXiv:1502.05635 [hep-th]].

[73] S. A. H. Mansoori, B. Mirza, A. Mokhtari, F. L. Dezaki and Z. Sherkatghanad, arXiv:1602.07245 [hep-th].

[74] M. Brigante, H. Liu, R. C. Myers, S. Shenker and S. Yaida, Phys. Rev. D **77**, 126006 (2008) [arXiv:0712.0805 [hep-th]].

[75] M. Brigante, H. Liu, R. C. Myers, S. Shenker and S. Yaida, Phys. Rev. Lett. **100**, 191601 (2008) [arXiv:0802.3318 [hep-th]].